Appl. Comput. Math., Vol.24, No.3, 2025, pp.469-485
DOI: 10.30546/1683-6154.24.3.2025.469

SOLVING THE EXACT NONLINEAR CONSOLIDATION EQUATION USING CHEBYSHEV CARDINAL FUNCTIONS

A. HAVVAEI[1], R.G. EJLALI[1,*], M. LAKESTANI[2,3,4,5], F.B. SARAND[1]

Abstract. The governing equation for the consolidation phenomenon inherently exhibits nonlinearity due to the dependence of the consolidation coefficient on parameters such as permeability and compressibility coefficients, which vary with both time and space. This study proposes the utilization of the Chebyshev Cardinal Functions (CCF) method for accurate solution of the given equation. A comparative analysis of the results, in conjunction with experimental observations and traditional methods, underscores the method's remarkable precision. The evaluation of efficiency employs the Nash Sutcliffe coefficient, yielding an average Nash-Sutcliffe Efficiency (NSE) coefficient of 0.98 - a clear indication of excellent performance. In comparison to Terzaghi and finite difference methods, the proposed approach exhibits efficiency enhancements of 2.6 and 130%, respectively. Furthermore, this study introduces a continuous mathematical solution that aligns with the underlying physics of the problem, diverging from the discrete solutions offered by approximate and linear methods.

Keywords: Consolidation Coefficient, Permeability, Compressibility, Chebyshev Cardinal Functions, Collocation Method.

AMS Subject Classification: 65M70, 65N35, 65M06.

1. Introduction

Based on the law of mass conservation and main assumptions including Darcy's law, saturation, homogeneity, isotropic soil behavior, and vertical drainage constraints, the governing equation of one-dimensional soil consolidation is presented, which is the basis of Terzaghi's consolidation theory in 1943 [42]. One of the most important assumptions in this equation is the constancy of the consolidation coefficient, C_v, during the soil consolidation process. This equation has been used linearly for a long time. The assumption that the consolidation coefficient remains constant in this equation is not inherently correct due to the changes of parameters affecting it such as permeability and compressibility coefficients during the consolidation process. In reality, the value of the consolidation coefficient changes with variations in the volumetric compressibility and permeability coefficients (m_v and k) during consolidation. Additionally, methods of experimental curves used to measure the consolidation coefficient provide different values for C_v for the same test data. These limitations result in a lack of confidence in the prediction of the consolidation rate [1].

A good reasonable estimate of the C_v requires an assessment of the rate of deformation/settlement of the clay soil due to loading. Terzaghi's theory for one-dimensional consolidation is the

[1]Department of Civil Engineering, Ta.C., Islamic Azad University, Tabriz, Iran
e-mail: Stu.Phd.Havvaei@iaut.ac.ir, Sarand@iau.ac.ir
[2]Department of Pure and Applied Mathematics, Saveetha School of Engineering, Saveetha Institute of Medical and Technical Sciences (SIMATS), Chennai - 602 105, Tamilnadu, India, e-mail: Lakestani@gmail.com
[3]Research Center of Performance and Productivity Analysis, Istinye University, Istanbul, Türkiye
[4]Faculty of Mathematics, Statistics and Computer Science, University of Tabriz, Tabriz, Iran
[5]Jadara University Research Center, Jadara University, Jordan
[*]Corresponding author e-mail: R.Ejlali@iau.ac.ir
Manuscript received 08 May 2025.

working basis of existing methods of measuring C_v. The consolidation coefficient is generally estimated from the time-deformation data (t-d) obtained from the one-dimensional consolidation test. Many researchers have tried to measure C_v from t-d data based on the curve fitting procedures. Basically, the curve fitting procedure uses the facilities related to the specifications of the theoretical relationships of the degree of consolidation (U) and the time factor (T) that are obtained from the experimental data. It is worth noting that the value of C_v obtained from experimental t-d data may be affected by primary (immediately after loading) or secondary compression [40]. In [39], the authors emphasized that primary compaction increases the value of C_v calculated by t-d data and secondary compaction decreases it. However, the authors showed that the rectangular hyperbola method and Asaoka's method can provide good predictions of C_v and end of primary compression (EOP) and are also useful tools for consolidation monitoring in site in [41]. All the methods mentioned above are presented based on the relationship of the consolidation equation, and in most scientific books, Terzaghi's one-dimensional consolidation equation was usually solved linearly using the finite difference method.

In recent decades, several researchers to illustrate the non-linear reality of this phenomenon have endeavored to forecast the soil consolidation coefficient using alternative behavioral parameters [7, 31]. Based on the relationship between e and $\log p$, the authors of [11] proposed the assumption that k_v/m_v and C_v remain constant with increasing pressure and developed the theory of non-linear consolidation for the first time. Other researchers have attempted to present a more realistic nonlinear theory by incorporating the variable consolidation coefficient and proposing various numerical methods [3, 12, 16, 22, 25, 35, 47, 49].

Including, the authors of [16] have tried to provide a more realistic nonlinear theory by neglecting the weight of the sample, considering creep in a confined layer of soil, and also considering the variable permeability and compressibility. They presented the results of their work based on the relationship between the degree of consolidation and the time factor. In this method, deformations are presumed to be small, thus settlement increases with rising vertical strain under the influence of increasing load. Their research delves into the impact of C_c/M ratio on consolidation rate [16]. In [40], the authors asserted that the soil consolidation coefficient is contingent upon its shrinkage index, I_s. They also established the relationship C_v as a function of I_s. In [49], the authors also tackled the consolidation equation semi-analytically by considering permeability and compressibility as variables. Similar to the paper [16], their approach involved C_v being variable based on degree of consolidation and the time factor. Consequently, limitations persist regarding the measurement of C_v.

In [1], the authors introduced the finite difference method for the semi-analytical solution of the nonlinear consolidation equation, considering variable permeability and compressibility based on the linear relationship between e-$\log \sigma'_v$ and e-$\log k$. The authors of [33] proposed a curve fitting method to calculate C_v using the relationship between the degree of dissipation at the base of sample (U_b) against $\log t$, highlighting the minor impact of secondary compression. In [21], the authors presented a straightforward mathematical approach for Asaoka's method applicable to settlement data acquired from one-dimensional consolidation tests. Utilizing Fredlund's one-dimensional consolidation theory, as well as Darcy's law and the authors developed a semi-analytical solution for the consolidation of unsaturated soils in the presence of free drainage wells [30]. In [34], the author resolved Terzaghi's one-dimensional consolidation equation by employing the wave propagation equation in one dimension, through the Fourier-Laplace equations and D'Alembert's solution. In [48], the authors addressed the consolidation equation of unsaturated soil with sand drainage using the differential quadrature method. Their research employed the differential quadrature method (DQM) method to solve partial differential equations using Lagrange polynomials. The author of [5] has presented solutions for one-dimensional consolidation of two-layered and multi-layered soils with impeded boundary drainage conditions under time-dependent loadings [5,8]. Conversely, the authors have introduced impeded drainage boundary conditions as special cases, combining permeability and incompressibility at the top and bottom of the soil layer in a multilayer system [15]. The authors provided an analytical solution for one-dimensional consolidation of a soil layer under ramp loading with exponentially time-growing drainage (ETGD) conditions, and compared it with Schiffman's solution [36]. Subsequently, research has been carried out on consolidation theory involving drainage boundary conditions that exponentially time-growing. This research has covered saturated soils with both single [20] and multiple layers [17] as well as unsaturated soils with single layer [44].

Also in recent decades, fractional differential equations have gained much attention due to the exact description of nonlinear phenomena and physical phenomena such as damping laws, electromagnetic, acoustics, viscoelasticity, electroanalytical chemistry, neuron modeling, diffusion processing, and material sciences [4,10]. In recent years, some attempts have been made to find analytical and numerical solutions for the fractional problems. Numerical and analytical methods have included the finite difference method [19], the Adomian decomposition method [23,24], the variational iteration method [28], the homotopy perturbation method [29], the homotopy analysis method [13], and other methods [9,18,27,37,38,43,46]. Today, in the field of geotechnical engineering, the necessity of providing a mathematical solution with appropriate accuracy to solve the consolidation equation in a non-linear form is highly needed. In this article, a numerical technique for solving parabolic partial differential equations with variable coefficients without simplifying assumptions such as given in [45]. The method is derived by expanding the required approximate solution as the elements of Chebyshev cardinal functions [2,14]. Using the operational matrix of derivative, the problem can be reduced to a set of algebraic equations. From the computational point of view, the solution obtained by this method is in excellent agreement with those obtained by previous works and also it is efficient to use.

2. The nonlinear governing equation

By recalling relation (1) from [1] and assuming the conditions used in the aforementioned article, the Eqn. (1) - a completely non-linear partial differential equation with a high degree of derivability - is presented as follows:

$$\frac{\partial u}{\partial t} = c_n(\sigma_t - u)^\alpha \frac{\partial^2 u}{\partial z^2}, \tag{1}$$

subject to the boundary and initial conditions:

$$u(0,t) = 0, \quad u(2H,t) = 0, \tag{2}$$

$$u(z,0) = u_0 = \sigma_t. \tag{3}$$

2.1. **Chebyshev cardinal functions.**

The N-th order Chebyshev cardinal functions over the range $[-1,1]$ are formally defined as following [2,7,16]:

$$C_j(x) = \frac{T_{N+1}(x)}{T_{N+1,x}(x_j)(x - x_j)}, \quad j = 1,2,\ldots,N+1, \tag{4}$$

where $T_{N+1}(x)$ is the Chebyshev polynomial of the second kind:

$$T_{N+1}(x) = \cos((N+1)\arccos(x)).$$

The points x_j are the roots of $T_{N+1}(x)$:

$$x_j = \cos\left(\frac{2j-1}{2N+2}\pi\right), \quad j = 1,2,\ldots,N+1.$$

Introducing the transformation $t = H(x+1)$, we approximate any function $g(t)$ over $[0,2H]$ as:

$$g(t) \approx \sum_{j=1}^{N+1} g(t_j)C_j(t) = G^T\Phi_N(t), \tag{5}$$

where t_j, $j = 1, 2, \ldots, N+1$, are the shifted points of x_j, $j = 1, 2, \ldots, N+1$, obtained by the transformation $t = H(x+1)$. Here, the points t_j are chosen such that $t_1 < t_2 < \cdots < t_{N+1}$ and

$$G = [g(t_1), g(t_2), \ldots, g(t_{N+1})]^T, \quad \Phi_N(t) = [C_1(t), C_2(t), \ldots, C_{N+1}(t)]^T. \tag{6}$$

2.2. **The operational matrix of derivative.** The derivative of vector Φ_N in (6) is:

$$\Phi'_N = D\Phi_N, \tag{7}$$

where D is the operational matrix of derivative. Let

$$\Phi'_N(t) = \left[C'_1(t), C'_2(t), \ldots, C'_{N+1}(t)\right]^T.$$

Using (5), we write:

$$C'_j(t) = \sum_{k=1}^{N+1} C'_j(t_k)C_k(t). \tag{8}$$

Hence,

$$D = \begin{bmatrix} C'_1(t_1) & \cdots & C'_1(t_{N+1}) \\ \vdots & \ddots & \vdots \\ C'_{N+1}(t_1) & \cdots & C'_{N+1}(t_{N+1}) \end{bmatrix}. \tag{9}$$

To compute $C'_j(t_k)$, we use:

$$\frac{T_{N+1}(t)}{t - t_j} = \beta \prod_{\substack{k=1 \\ k \neq j}}^{N+1} (t - t_k), \tag{10}$$

where $\beta = \frac{2^N}{H^{N+1}}$. Differentiating (10):

$$\frac{d}{dt}\left(\frac{T_{N+1}(t)}{t - t_j}\right) = \beta \times \sum_{\substack{i=1 \\ i \neq j}}^{N+1} \prod_{\substack{k=1 \\ k \neq i,j}}^{N+1} (t - t_k) = \sum_{\substack{i=1 \\ i \neq j}}^{N+1} \frac{T_{N+1}(t)}{(t - t_j)(t - t_i)}. \tag{11}$$

Thus,

$$C'_j(t) = \frac{1}{T_{N+1,x}(t_j)} \sum_{\substack{i=1 \\ i \neq j}}^{N+1} \frac{T_{N+1}(t)}{(t - t_j)(t - t_i)} = \sum_{\substack{i=1 \\ i \neq j}}^{N+1} \frac{1}{t - t_i} C_j(t). \tag{12}$$

For $j = k$:

$$C'_j(t_j) = \sum_{\substack{i=1 \\ i \neq j}}^{N+1} \frac{1}{t_j - t_i}, \tag{13}$$

and for $j \neq k$:

$$C'_j(t_k) = \frac{\beta}{T_{N+1,t}(t_j)} \prod_{\substack{l=1 \\ l \neq k,j}}^{N+1} (t_k - t_l). \tag{14}$$

2.3. **Description of numerical method using Chebyshev cardinal functions with Crank-Nicolson time stepping.** This section focuses on resolving the Eqn. (1) accompanied by the boundary and initial conditions specified in (2) and (3) using Chebyshev cardinal functions over the interval $[0, 2H]$.

Integrating (1) over $[t, t + \delta t]$ gives:

$$u(z, t + \delta t) - u(z, t) = \int_t^{t+\delta t} c_n(\sigma_t - u(z, t))^\alpha u_{zz}(z, t) dt. \tag{15}$$

Using trapezoidal rule:

$$u(z,t+\delta t)-u(z,t)\approx\frac{\delta t}{2}\left[c_n(\sigma_t-u(z,t))^{\alpha}u_{zz}(z,t)+c_n(\sigma_t-u(z,t+\delta t))^{\alpha}u_{zz}(z,t+\delta t)\right], \quad (16)$$

where δt is the time step size. Denoting $u^m=u(z,t^m)$ and $t^m=t^{m-1}+\delta t$, we write:

$$u^{m+1}-u^m=\frac{\delta t}{2}\left[c_n(\sigma_t-u^m)^{\alpha}\nabla^2u^m+c_n(\sigma_t-u^{m+1})^{\alpha}\nabla^2u^{m+1}\right]. \quad (17)$$

The operator ∇ signifies the gradient. Using (5) and (7):

$$u^m=u(z,t^m)=\sum_{j=1}^{N+1}u_j^mC_j(z)=U_m^T\Phi_N(z),\quad m=0,1,2,\ldots \quad (18)$$

$$\nabla^2u^m=U_m^T\frac{d^2}{dz^2}\Phi_N(z)=U_m^TD\frac{d}{dz}\Phi_N(z)=U_m^TD^2\Phi_N(z). \quad (19)$$

where $U_m=[u_1^m,u_2^m,\ldots,u_{N+1}^m]^T$. Substituting into (17):

$$\begin{aligned}U_{m+1}^T\Phi_N(z)-\frac{\delta t}{2}c_n(\sigma_t-U_{m+1}^T\Phi_N(z))^{\alpha}U_{m+1}^TD^2\Phi_N(z)\\=U_m^T\Phi_N(z)+\frac{\delta t}{2}c_n(\sigma_t-U_m^T\Phi_N(z))^{\alpha}U_m^TD^2\Phi_N(z).\end{aligned} \quad (20)$$

Using boundary condition that was given in (2):

$$U_{m+1}^T\Phi_N(0)=0,\quad U_{m+1}^T\Phi_N(2H)=0. \quad (21)$$

Applying (20) at points t_j, $j=2,\ldots,N$ and using $\Phi_N(t_j)=e_j$, where $\mathbf{e}_j$ denotes the j^{th} column of the $N\times N$ identity matrix, leading to the following expression:

$$\begin{aligned}u_j^{m+1}-\frac{\delta t}{2}c_n(\sigma_t-u_j^{m+1})^{\alpha}U_{m+1}^TD_j^2=u_j^m+\frac{\delta t}{2}c_n(\sigma_t-u_j^m)^{\alpha}U_m^TD_j^2.\\ j=2,3,N,\quad m=0,1,2.\end{aligned} \quad (22)$$

Here, D_j^2 is the j-th column of D^2. The Eqns. (21) and (22) with initial condition that was given in (3) form a system of $N+1$ algebraic equations for unknowns U_m at each time step m. Consequently, the unknown functions $u^m(z)$ can be determined using the relation (18).

3. Theoretical stability of the linearized scheme

We consider the notion of asymptotic stability for a numerical technique as outlined in [6] for a discrete problem described as:

$$\frac{dU}{dt}=LU, \quad (23)$$

where L is considered to be a diagonalizable matrix.

Definition 1. The absolute stability region of a numerical method is defined for the scalar model problem:

$$\frac{dU}{dt}=\lambda U, \quad (24)$$

as the collection of all $\lambda\delta t$ such that $\|U_m\|$ remains bounded as $t\to\infty$. A numerical method is deemed asymptotically stable for a specific problem if, for sufficiently small $\delta t>0$, the product of δt and each eigenvalue of L falls within the absolute stability region [32].

Regarding the Crank–Nicolson scheme, it exhibits absolute stability across the entirety of the left-half plane.

3.1. **Stability for linearized governing equation.** We consider the linearized governing equation:

$$\frac{\partial u}{\partial t} = c_n(\sigma_t - u)^\alpha \frac{\partial^2 u}{\partial z^2}, \tag{25}$$

where the linearization coefficient μ stands for values of u. We assume that $|\mu| \leq M$, where M is an upper bound of u. Here $L = \Gamma^{-1}\Lambda$, where Γ and Λ are matrices in the form:

$$\Gamma = (V_1, V_2, \dots, V_{N+1}), \quad \Lambda = (C_1, C_2, \dots, C_{N+1}), \tag{26}$$

where V_i and C_i, $i = 1, 2, \dots, N+1$, are the vectors:

$$V_i = \Phi_N(z_i), \quad i = 1, 2, \dots, N+1, \tag{27}$$

$$C_i = c_n(\sigma_t - u)^\alpha D^2\Phi_N(z_i), \quad i = 1, 2, \dots, N+1. \tag{28}$$

Thus, the discretized linearized governing equation becomes:

$$\frac{dU}{dt} = LU. \tag{29}$$

The Crank–Nicolson method exhibits A-stability. The absolute stability region for the Crank–Nicolson time-stepping approach is illustrated in Fig.1, for different values of α, c_n, and σ_t presented in the examples.

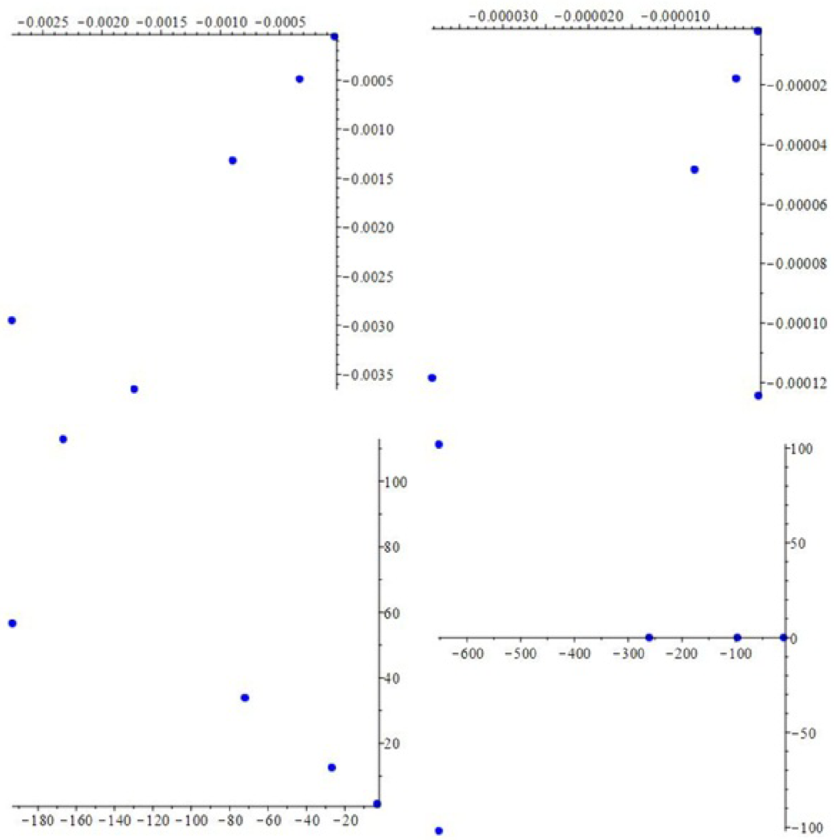

FIGURE 1. Eigenvalues of L: Top-left for $\alpha = 0.31$, top-right for $\alpha = 0.45$, bottom-left for $\alpha = -0.14$, and bottom-right for $\alpha = -0.60$.

4. Experimental studies

To evaluate and numerically solve the proposed equation, the authors conducted laboratory experiments on four distinct soil samples in [1]. The nonlinear parameters of these tested samples are documented in Table 1. As discussed in Section 2, it is assumed that the relationships between e–$\log k$ and e–$\log \sigma_v'$ are linear. The distance from the origin and the inclination of the e–$\log k$ line are denoted as b and M, respectively, while for the e–$\log \sigma_v'$ line, they are represented as a and C_c, respectively. These parameters are associated with soil permeability and compressibility.

Table 1. Non-linear parameters of samples [1].

Soil sample	Applied total stress σ_t (kPa)	Initial void ratio e_0	Compressibility characteristic		Permeability characteristic		Non-linearity coefficient	
			a	C_c	b	M	C_n	α
1	15	2.14	2.76	0.61	7.77	0.89	2.83E−06	0.31
2	30	1.00	1.52	0.32	5.14	0.58	8.41E−07	0.45
3	60	0.83	1.36	0.34	1.92	0.18	9.77E−04	-0.14
4	60	0.52	1.05	0.25	1.21	0.11	5.01E−02	-0.60

Based on the above nonlinear parameters, the Eqn. (1) was solved by the method mentioned in Section 2.

Here, we briefly present the method for Test Sample 1. In this case, we have:

$$\begin{aligned} u(z,0) &= u_0 = 15, \\ c_n &= 2.83 \times 10^{-6}, \\ \alpha &= 0.31. \end{aligned}$$

Using relation (18), we write:

$$u(z,0) = 15 = \sum_{j=1}^{N+1} u_j^0 C_j(z) = U_0^T \Phi_N(z),$$

so the entries of the vector U_0, using relation (5), are:

$$u_j^0 = 15.$$

To find the function $u(z,t)$ at time $t^1 = t^0 + \Delta t = \Delta t$, we use relation (22) and construct the following system of equations by setting $m = 0$:

$$u_j^1 - \frac{\delta t}{2} c_n (15 - u_j^1)^\alpha U_1^T D_j^2 = u_j^0 + \frac{\delta t}{2} c_n (\sigma_t - u_j^0)^\alpha U_0^T D_j^2, \quad j = 2, 3, \ldots, N. \tag{30}$$

Note that here only the values of the vector U_1 are unknown. Applying boundary conditions (21), we also have:

$$U_1^T \Phi_N(0) = 0, \quad U_1^T \Phi_N(2H) = 0. \tag{31}$$

The Eqns. (30) together with (31) form a system of $N+1$ algebraic equations with $N+1$ unknowns. Solving this system yields the vector U_1, and thus the value of the function $u(z,t)$ at time t^1 is obtained. Now, using $u(z,t^1)$ as the starting point, we can proceed similarly to compute $u(z,t^2)$, and so on.

5. Results

5.1. **Variation of pore water pressure with time and depth.** By promptly applying the load and initiating the consolidation process, the pore water pressure decreases gradually due to drainage. With two-way drainage conditions, changes in pore water pressure are also observed at different depths of the sample. The graph illustrating changes in pore water pressure relative to the sample depth and at various time intervals is depicted in Fig.2.

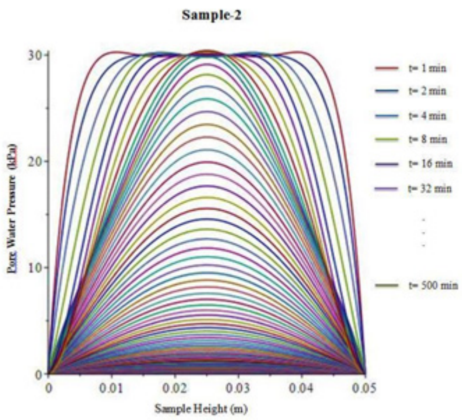

Figure 2. Diagram of pore water pressure changes at sample depth with different times.

By transforming the diagram in Fig.2 into a three-dimensional representation, the pore water pressure waterfall becomes visible. This waterfall effectively illustrates the process by which the solutions of Terzaghi's one-dimensional consolidation equation are situated within a non-linear category. Furthermore, this waterfall visually demonstrates the tangible variations in pore water pressure.

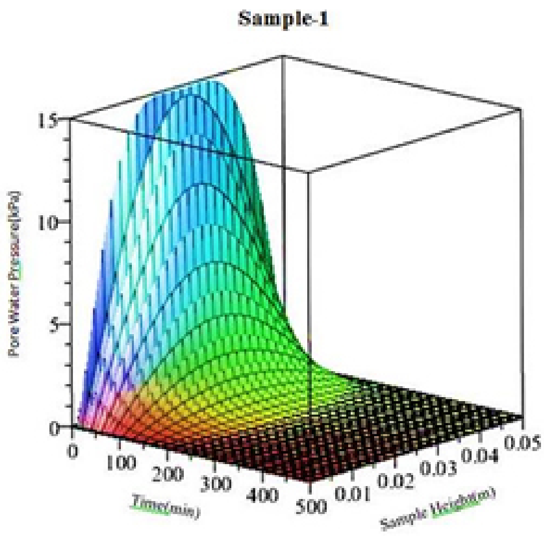

Figure 3. Pore pressure waterfall.

By focusing on Fig.3, we can readily comprehend and observe the variations in water pressure within the cavity. These changes span from the initial moment, characterized by the highest water pressure, to the point where the pressure head reaches zero. Additionally, the relationship between pore water pressure and the samples height-depicted as the width of the waterfall in Fig.3 is clearly illustrated. The title of the "pore water pressure cascade" and its distinctive shape enhance our understanding of pore water pressure fluctuations during the consolidation process.

5.2. **Time-settlement relationship.** This research re-examines the relationship between the average degree of consolidation and real time by eliminating the need to calculate the consolidation coefficient and the time factor, as previously developed by the authors of [1]. The presented graphs in Figs.4-7 are based on the results obtained from the proposed method in this study.

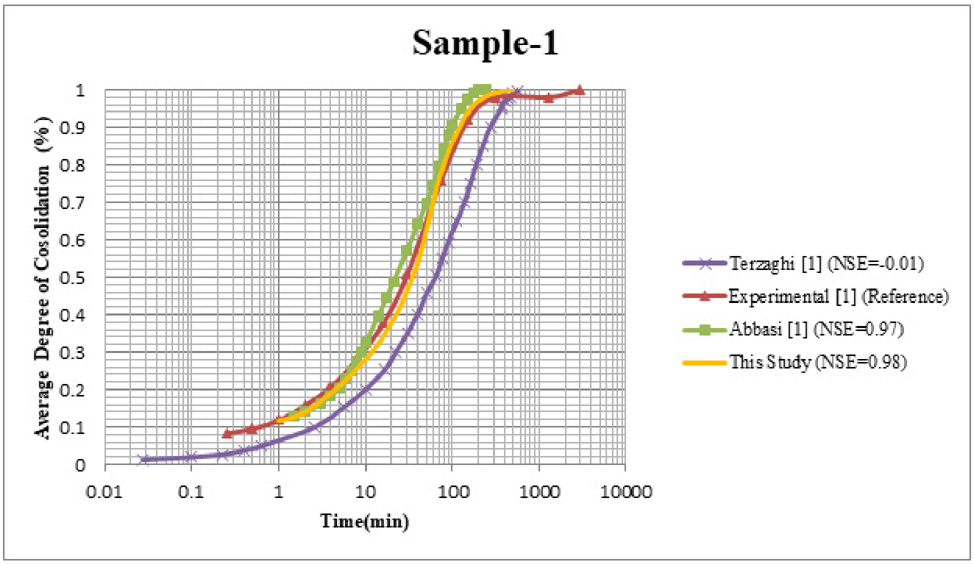

FIGURE 4. Soil sample 1, applied pressure 15 kPa.

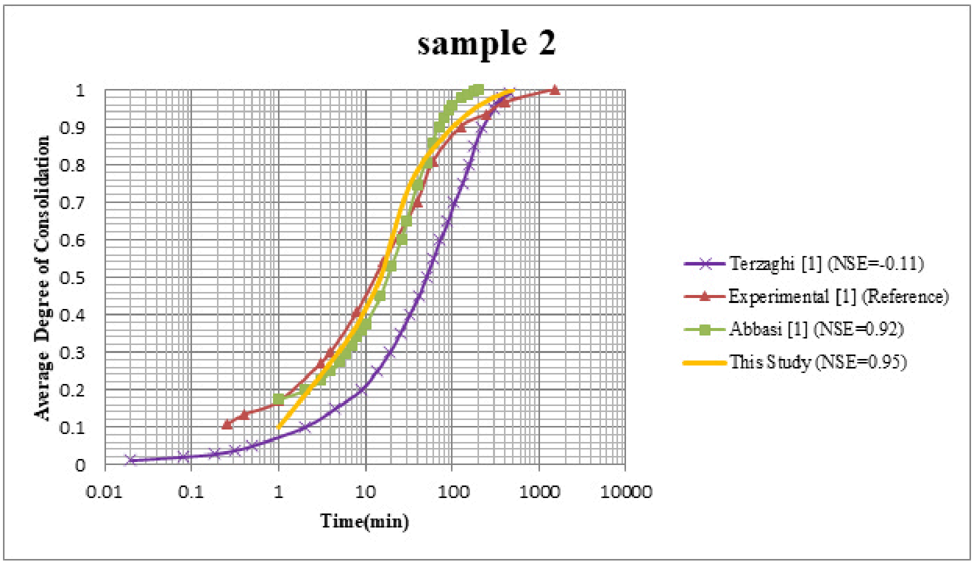

FIGURE 5. Soil sample 2, applied pressure 30 kPa.

Based on the diagrams in Figs.4-7, we draw the following conclusions:

- The proposed method in this research exhibits significantly greater accuracy compared to the finite difference method, yielding answers that closely align with laboratory values.

- The magnitude of the parameter α plays a crucial role in estimating the consolidation rate. Positive α values indicate a slower consolidation rate than predicted by Terzaghi's theory, while negative α conditions correspond to a faster consolidation rate. These findings corroborate the results obtained by the authors of [1].
- The proposed method for evaluating consolidation in the range of primary consolidation is more accurate than at the beginning of consolidation and during secondary consolidation. This method plays an important role in determining the time steps for solving the nonlinear equation.

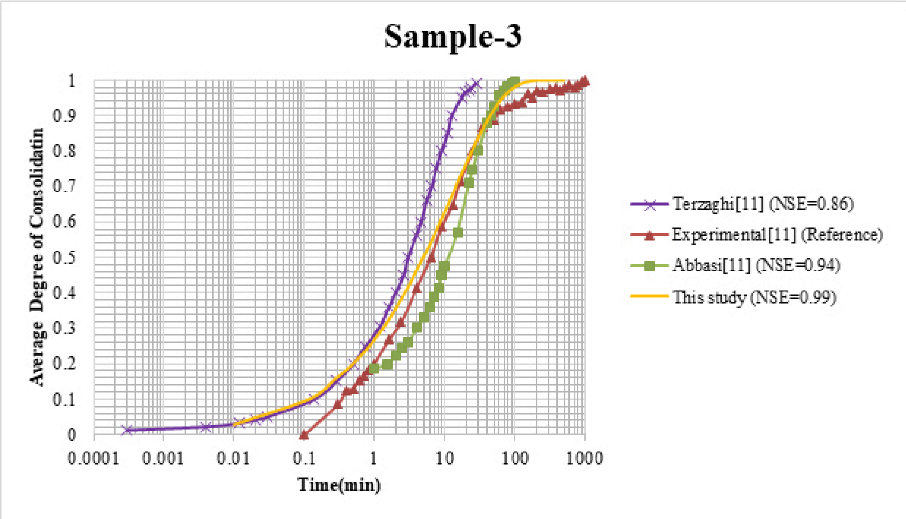

FIGURE 6. Soil sample 3, applied pressure 60 kPa.

- The relationship between the average degree of consolidation and real time was obtained as a polynomial function with a high correlation coefficient. This relationship can be presented as follows for Sample 1:

$$U(t) = -725.43t^6 + 3098.1t^5 - 5276.5t^4 + 4640t^3 - 2287.7t^2 + 635.97t + 14.967. \quad R^2 = 0.998. \tag{32}$$

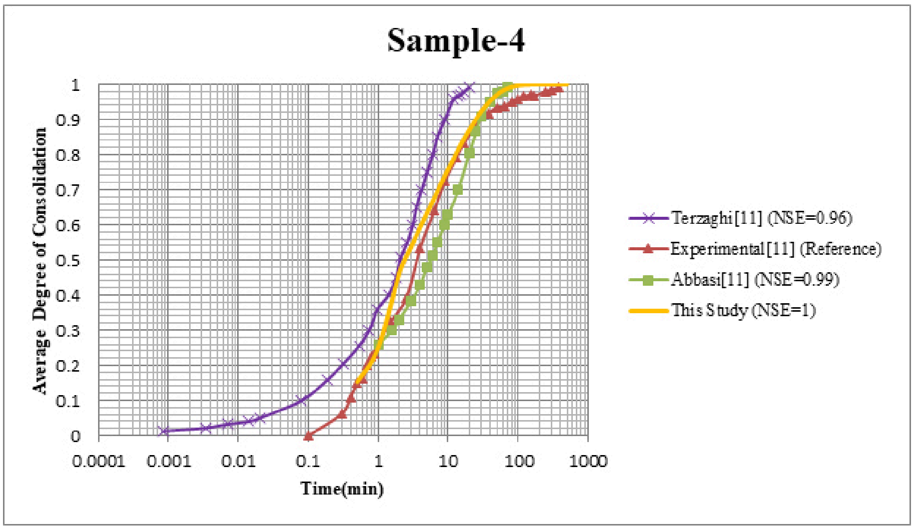

FIGURE 7. Soil sample 4, applied pressure 60 kPa.

By using Eqn. (32), without the need for additional calculations and measurements, it becomes easy to calculate the degree of consolidation at any desired time. The high correlation coefficient in the above relation ensures the accuracy of the average degree of consolidation obtained from this expression.

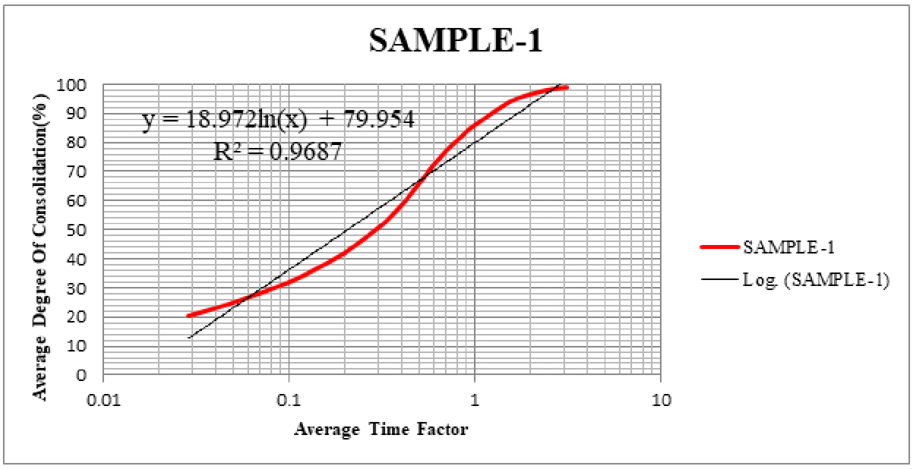

FIGURE 8. Variation of the average degree of consolidation with the time factor in the primary consolidation limit (soil sample 1).

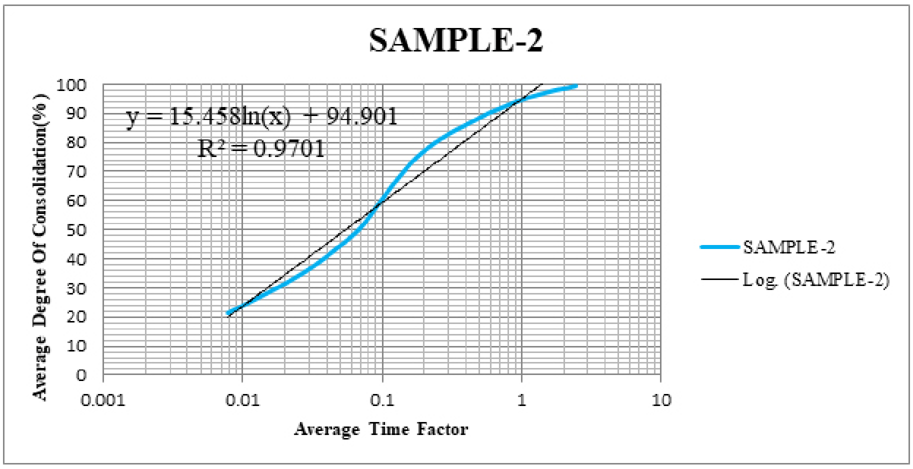

FIGURE 9. Variation of the average degree of consolidation with the time factor in the primary consolidation limit (soil sample 2).

5.3. **Determining the U–T relationship.** Despite the direct determination of the relationship between the average degree of consolidation and real time in the previous section, this section aims to compare the achievements of the proposed method with the results of other research. Specifically, we present the relationship between the average degree of consolidation and the time factor.

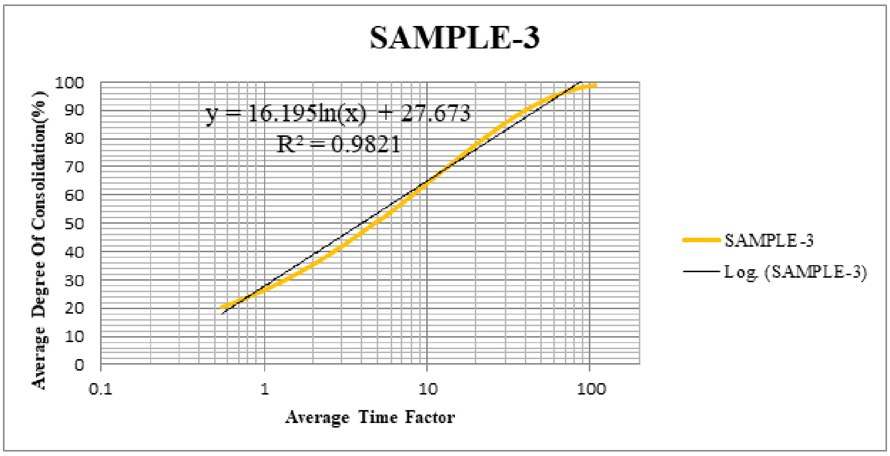

FIGURE 10. Variation of the average degree of consolidation with the time factor in the primary consolidation limit (soil sample 3).

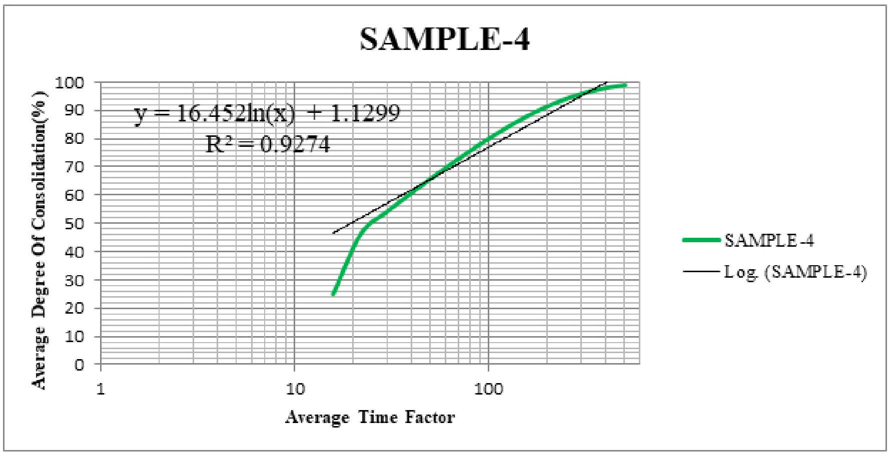

FIGURE 11. Variation of the average degree of consolidation with the time factor in the primary consolidation limit (soil sample 4).

Based on the graphs in Figs.8-11, we present the relationship between the average degree of consolidation and the time factor for each of the samples within the primary consolidation range:

$$U = 18.972\ln(T_v) + 79.954, \quad R^2 = 0.9687, \quad \text{Sample 1} \tag{33}$$

$$U = 15.458\ln(T_v) + 94.901, \quad R^2 = 0.9701, \quad \text{Sample 2} \tag{34}$$

$$U = 16.195\ln(T_v) + 27.673, \quad R^2 = 0.9821, \quad \text{Sample 3} \tag{35}$$

$$U = 16.452\ln(T_v) + 1.1299, \quad R^2 = 0.9274, \quad \text{Sample 4} \tag{36}$$

As evident from the data, the relationships in the Eqns. (33)–(36) depend on the initial characteristics of the samples and the applied stress level. However, it is not feasible to present a single universal relationship for all samples with acceptable accuracy.

The continuous nature of the consolidation process allows us to obtain these relations without the need for discretization. This approach aligns with the reality of the subject. In contrast, previous research often required graph discretization to illustrate the relationship between changes in the degree of consolidation and the time factor. Fortunately, our current study has addressed this issue.

5.4. **Evaluating the efficiency of the proposed method.** In this study, the Nash-Sutcliffe Efficiency (NSE) coefficient was used to optimize the objective function. This coefficient can be calculated from the following relationship:

$$\mathrm{NSE} = 1 - \frac{\sum_{i=1}^{n}(Q_{m,i} - Q_{s,i})^2}{\sum_{i=1}^{n}(Q_{m,i} - \overline{Q_m})^2},$$

where:

- n represents the number of observations.
- $Q_{m,i}$ and $Q_{s,i}$ denote the measured and estimated values of the degree of consolidation, respectively.
- $\overline{Q_m}$ is the average of the measured values of the degree of consolidation in the laboratory.

The numerical value of the NSE coefficient varies from negative infinity to 1, with 1 being the optimal value. A value closer to 1 indicates a better estimation method. Generally, if the Nash-Sutcliffe index is greater than 0.75, the models performance is considered excellent. If it falls between 0.5 and 0.75, it is considered satisfactory, while values below 0.5 are deemed unacceptable [26].

Table 2 presents the NSE coefficients for the Terzaghi method, the finite difference method, and the method proposed in this study. As observed, the proposed method achieves the highest NSE values across all samples, demonstrating its superior accuracy and excellent performance.

Table 2. The NSE coefficient for different methods.

Method	**Sample-1**	**Sample-2**	**Sample-3**	**Sample-4**
Terzaghi	-0.01	-0.11	0.86	0.96
Finite Difference (Abbasi et al. [1])	0.97	0.92	0.94	0.99
This Study	0.98	0.95	0.99	1.00

6. Discussion

In this paper, we presented a semi-analytical solution for the nonlinear equation of one-dimensional soil consolidation. This solution was directly derived by revisiting the equation developed by the authors of [1]. Notably, our proposed method exhibited greater accuracy compared to other existing methods.

One fundamental assumption in Terzaghi's consolidation theory pertains to the application of instantaneous load. However, the reaction of the sample due to this type of loading remains invisible in previously established solutions. In our novel approach, the response of the sample to the application of instantaneous load becomes evident, as illustrated in Fig.12.

In the regions indicated in Fig.12, during the initial moments of consolidation and upon the application of instantaneous load, the pore water pressure near the drainage boundaries exceeds the initial value and promptly returns to normal. This behavior reflects a weak impact resulting from instantaneous loading and demonstrates the elastic response of the sample environment.

In a multi-phase environment such as soil, the liquid phase exhibits continuity. As a result, the initial response originates from this part and manifests as a momentary increase in pore water pressure. In this context, the response of the gas phase is disregarded due to its insignificance.

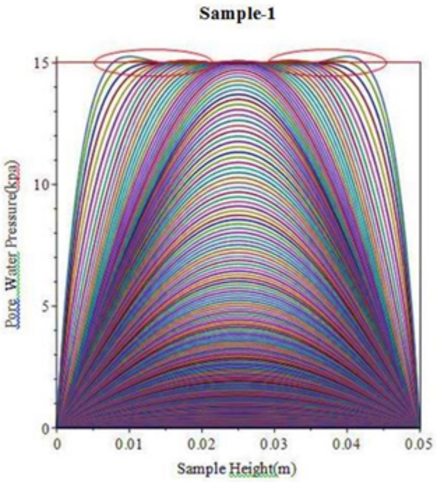

Figure 12. Specimen response to instantaneous loading.

One of the distinctive advantages of the method presented in this paper lies in its ability to predict the environmental response under applied conditions. This prediction aligns with the observed reality of the tested phenomenon, which is frequently overlooked in laboratory measurements. The emphasis on this aspect within the proposed solution aims to demonstrate the accuracy of the method put forth in this article.

7. Conclusion

In this study, we presented a novel semi-analytical solution for the non-linear Terzaghi consolidation equation using the Chebyshev Cardinal Functions (CCF). Additionally, we employed the combined spectral–finite difference method for numerical solution.

The integration of combined methods in solving equations represents a recent approach that enhances solution accuracy. Based on the results obtained in the present study, the following results can be presented:

- The variable consolidation coefficient is linked to effective stress through two parameters, α and C_n.
- The predicted consolidation, when compared to that obtained from Terzaghi's theory, depends on the numerical value of the exponent α in the Eqn. (1). Specifically, for positive values of α, the predicted consolidation is slower than Terzaghi's theory, while the opposite holds true.
- For smaller $|\alpha|$ values, the consolidation speed in the initial consolidation range closely aligns with the laboratory results.
- Accurate determination of the time steps in the numerical method results is crucial. Failure to properly adjust these steps can lead to method instability.
- Laboratory results have been utilized to determine appropriate time steps.
- The proposed semi-analytical method, along with the combined numerical method used in this research, exhibits relatively high accuracy. As a result, it can effectively simulate the response of non-continuous environments under applied conditions.
- The relationship between the average degree of consolidation and real time was determined without the need to measure the consolidation coefficient or discretize the equation with high accuracy.
- One of the prominent features of the proposed method is that it does not require discretization for relationships with continuous nature.

- Slight deviations between experimental and theoretical results may arise from inconsistencies in experimental settings and theoretical assumptions. Additionally, the effect of the creep phenomenon on experimental results is likely.
- In the context of laboratory consolidation, the measured permeability tends to be larger than the actual value due to water leakage from the space between the sample and the mold. This unintended effect results in a faster settlement rate compared to the theoretical results.
- The semi-analytical solution stands out as a highly effective method for solving challenging consolidation problems, especially when considering variable compressibility and permeability.
- The proposed method demonstrates excellent efficiency based on the NSE criterion. It yields more accurate results compared to other methods, making it highly effective for estimating the rate of consolidation.
- Stability for the linearized governing equation, according to the Crank–Nicolson scheme, is A-stable.

References

[1] Abbasi, N., Rahimi, H., Javadi, A.A., Fakher, A. Finite difference approach for consolidation with variable compressibility and permeability, *Comput. Geotech.*, Vol.34, No.1, 2007, pp.41-52.

[2] Afarideh, A., Saei, F.D., Lakestani, M., Saray, B.N. Pseudospectral method for solving fractional Sturm-Liouville problem using Chebyshev cardinal functions, *Phys. Scr.,* Vol.96, No.12, 2021, p.125267.

[3] Akbarov, S.D., Bagirov, E.T., Sardarova, I.Z. The response of an infinite elastic medium with inhomogeneous initial stresses to moving load acting in a cylindrical cavity, *Appl. Comput. Math.*, Vol.24, No.1, 2025, pp.3-15.

[4] Beyer, H., Kempfle, S. Definition of physically consistent damping laws with fractional derivatives, *Z. Angew. Math. Mech.*, Vol.75, No.8, 1995, pp.623-635.

[5] Cai, Y.Q., Liang, X., Wu, S.M. One-dimensional consolidation of layered soils with impeded boundaries under time-dependent loadings, *Appl. Math. Mech. Eng.*, Vol.25, No.8, 2004, pp.937-944.

[6] Canuto, C., Hussaini, M.Y., Quarteroni, A., Zang, T.A. *Spectral Method in Fluid Dynamics*, Springer-Verlag, Berlin, Vol.30, No.4, 1988, 568 p.

[7] Cao, W., Rehman, S.U., Asjad, M.I., Inc, M. Numerical study of bioconvection and Cattaneo-Christov heat flux model in MHD Maxwell nanofluid flow over a variable thickness elastic surface, *Appl. Comput. Math.*, Vol.23, No.2, 2024, pp.182-200.

[8] Carrier, W.D. Consolidation parameters derived from index tests, *Geotechnique*, Vol.35, No.2, 1985, pp.211-213.

[9] Chen, R.P., Zhou, W.H., Wang, H.Z., Chen, Y.M. One-dimensional nonlinear consolidation of multi-layered soil by differential quadrature method, *Comput. Geosci.*, Vol.32, No.5, 2005, pp.358-369.

[10] Daftardar-Gejji, V., Jafari, H. Analysis of a system of nonautonomous fractional equations involving Caputo derivatives, *J. Math. Anal. Appl.*, Vol.328, No.1, 2007, pp.26-33.

[11] Davis, E.H., Raymond, G.P. A Non-linear theory of consolidation, *Geotechnique*, Vol.15, No.2, 1965, pp.161-173.

[12] Gibson, R.E., England, G.L., Hussey, M.J.L. The theory of one-dimensional consolidation of saturated clays, *Geotechnique*, Vol.17, No.3, 1967, pp.261-273.

[13] Hashim, I., Abdulaziz, O., Momani, S. Homotopy analysis method for fractional IVPs, *Commun. Nonlinear Sci. Numer. Simul.*, Vol.14, No.3, 2009, pp.674-684.

[14] Lakestani, M., Dehghan, M. Numerical solution of fourth-order integro-differential equations using Chebyshev cardinal functions, *Inter. J. Comput. Math.*, Vol.87, No.6, 2010, pp.1389-1394.

[15] Lee, P.K.K., Xie, K.H., Cheung, Y.K. A study on one-dimensional consolidation of layered systems, *Int. J. Numer. Anal. Methods Geomech.*, Vol.16, No.11, 1992, pp.815-831.

[16] Lekha, K.R., Krishnaswamy, N.R., Basak, P. Consolidation of clays for variable permeability and compressibility, *Geotech. Geoenviron. Eng.*, Vol.129, No.11, 2003, pp.1001-1009.

[17] Liu, J.C., Lei, G.H. One-dimensional consolidation of layered soils with exponentially time-growing drainage boundaries, *Comput. Geotech.*, Vol.54, 2012, pp.202-209.

[18] Liu, S., Luan, Z., Kabanikhin, S.I., Strijhak, S.V., Zhang, Y. Solving a type of nonlinear Schrödinger equations using a physically informed neural network and tuning the adaptive activation function, *TWMS J. Pure Appl. Math.*, Vol.15, No.2, 2024, pp.203-227.

[19] Meerschaert, M.M., Tadjeran, C. Finite difference approximations for two-sided space-fractional partial differential equations, *Appl. Numer. Math.*, Vol.56, 2006, pp.80-90.

[20] Mei, G.X., Chen, Q.M. Solution of Terzaghi one-dimensional consolidation equation with general boundary conditions, *J. Cent. South. Univ.*, Vol.20, No.8, 2013, pp.2239-2244.

[21] Mesri, G., Huvaj-Sarihan, N. The Asaoka method revisited, *Proc. 17th Int. Conf. on Soil Mech. Geotech. Eng.*, Alexandria, Egypt, Vol.1, 2009, pp.131-134.

[22] Mesri, G., Rokhsar, A. Theory of consolidation for clays, *ASCE J. Geotech. Eng. Div.*, Vol.100, No.8, 1974, pp.889-904.

[23] Momani, S., Al-Khaled, K. A numerical solution for systems of fractional differential equations by the decomposition method, *Appl. Math. Comput.*, Vol.162, No.3, 2005, pp.1351-1365.

[24] Momani, S., Odibat, Z. Analytical solution of a time-fractional Navier-Stokes equation by Adomian decomposition method, *Appl. Math. Comput.*, Vol.177, 2006, pp.488-494.

[25] Morris, P.H. Analytical solution of linear finite-strain one-dimensional consolidation, *J. Geotech. Geoenviron. Eng.*, Vol.128, No.4, 2002, pp.319-326.

[26] Nash, J.E., Sutcliffe, J.V. River flow forecasting through conceptual models part 1 – a discussion of principles, *J. Hydrology*, Vol.10, No.3, 1970, pp.282-290.

[27] Nourian, F., Lakestani, M., Sabermahani, S., Ordokhani, Y. Touchard wavelet technique for solving time-fractional Black–Scholes model, *Comput. Appl. Math,* Vol.41, No.4, 2022, p.150.

[28] Odibat, Z., Momani, S. Application of variational iteration method to nonlinear differential equations of fractional order, *Int. J. Nonlinear Sci. Numer. Simul.,* Vol.7, No.1, 2006, pp.27-34.

[29] Odibat, Z., Momani, S. Modified homotopy perturbation method: application to quadratic Riccati differential equation of fractional order, *Chaos Soliton. Fract.,* Vol.36, No.1, 2008, pp.167-174.

[30] Qin, A.F., Sun, D.A., Yang, L.P., Weng, Y.F. A semi-analytical solution to consolidation of unsaturated soils with the free drainage well, *Comput. Geotech.,* Vol.37, 2010, pp.867-875.

[31] Raju, N., Pandian, P.S.R., Nagaraj, T. Analysis and estimation of coefficient of consolidation, *Geotech. Testing J.,* Vol.18, No.2, 1995, pp.252-258.

[32] Rathish Kumar, B.V., Mehra, M. A wavelet Taylor Galerkin method for parabolic and hyperbolic partial differential equations, *Int. J. Comput. Methods,* Vol.2, No.1, 2005, pp.75-97.

[33] Robinson, R.G., Soundra, B. Coefficient of consolidation from midplane pore pressure measurements, *Int. J. Geotech. Eng.,* Vol.2, No.4, 2008, pp.417-423.

[34] Romolo, D.F. Exact solution to Terzaghi's consolidation equation, arXiv preprint, 2011; arXiv:1102.2060.

[35] Sadek, L., Yüzbasi, S., Alaoui, H.T. Two numerical solutions for solving linear and nonlinear systems of differential equations, *Appl. Comput. Math.,* Vol.23, No.4, 2024, pp.421-436.

[36] Schiffman, R.L. Consolidation of soil under time-dependent loading and varying permeability, *Proc. Highway Research Board,* Vol.37,1958, pp.584-617.

[37] Shafinejhad, Z., Zarebnia, M. Numerical solution of fractional Volterra integro-differential equations using flatlet oblique multiwavelets, *Comput. Meth. Diff. Equ.,* Vol.12, No.2, 2024, pp.374-391.

[38] Singh, A., Kumar, S., Ramos, H. An efficient computational method based on exponential B-splines for a class of fractional sub-diffusion equations, *Comput. Meth. Diff. Equ.,* Vol.12, No.4, 2024, pp.719-740.

[39] Sridharan, A., Murthy, N.S., Prakash, K. Rectangular hyperbola method of consolidation analysis, *Geotechnique,* Vol.37, No.3, 1987, pp.355-368.

[40] Sridharan, A., Nagaraj, H.B. Coefficient of consolidation and its correlation with index properties of remoulded soils, *Geotech. Testing J.,* Vol.27, No5, 2004, pp.469-474.

[41] Tan, S.A., Chew, S.H. Comparision of the hyperbolic and Asaoka observational method of monitoring consolidation with vertical drains, *Soils Found.,* Vol.36, No.3, 1996, pp.31-42.

[42] Terzaghi, K. *Theoretical Soil Mechanics*, John Wiley & Sons, New York, 1943, 510 p.

[43] Valizadeh, M., Mahmoudi, Y., Dastmalchi Saei, F. On fractional linear multi-step methods for fractional order multi-delay nonlinear pantograph equation, *Comput. Meth. Diff. Equ.,* Vol.12, No.3, 2024, pp.511-522.

[44] Wang, L., Sun, D., Qin, A. Semi-analytical solution to one-dimensional consolidation for unsaturated soils with exponentially time-growing drainage boundary conditions, *Int. J. Geomech.,* Vol.18, No.2, 2018, 04017144.

[45] Xie, K.H., Xie, X.Y., Jiang, W. A study on one-dimensional nonlinear consolidation of double layered soil, *Comput. Geotech.,* Vol.29, No.2, 2002, pp.151-168.

[46] Xu, H. Y., Aljohani, A., Xu, Y.H., Li, H., Shali, J.A. Results on solutions for several systems of the first order nonlinear PDEs and PDDEs in C2, *TWMS J. Pure Appl. Math.,* Vol.15, No.2, 2024, pp.228-245.

[47] Yucel, M., Mukhtarov, O.Sh. A new algorithm for solving two-linked boundary value problems with impulsive conditions, *TWMS J. Pure Appl. Math.,* Vol.15, No.2, 2024, pp.174-182.

[48] Zhou, W.H., Tu, S.H. Unsaturated consolidation in a sand drain foundation by differential quadrature method,*Procedia Earth Planet. Sci.,* Vol.5, 2012, pp.52-57.

[49] Zhuang, Y.C., Xie, K.H., Li, X.B. Nonlinear analysis of consolidation with variable compressibility and permeability, *J. Zhejiang Univ. Sci. A.* Vol.6, No.3, 2005, pp.181-187.

Arash Havvaei - is a Ph.D. degree candidate in Geotechnical Engineering in the Department of Civil Engineering at Tabriz Branch, Islamic Azad University, Tabriz, Iran. He received his M.Sc. degree in Geotechnical Engineering from the University of Tabriz in 2013. His research focuses on soil consolidation, image processing, physical and numerical modeling, and the setup of soil mechanics tests.

Reza G. Ejlali - is currently an Assistant Professor in the Department of Civil Engineering at Tabriz Branch, Islamic Azad University, Tabriz, Iran. He received his M.Sc. degree in Civil Engineering from Iran University of Science and Technology in 1993 and Ph.D. degree in Civil Engineering from the University of Tabriz in 2010. His research interests include simulations, optimizations, and numerical methods.

Mehrdad Lakestani -is currently a Full Professor in the Department of Applied Mathematics at the University of Tabriz, Tabriz, Iran. He received his M.Sc. and Ph.D. degrees in Applied Mathematics from Amirkabir University of Technology, Iran in 2000 and 2005, respectively. His research interests include spectral methods, wavelets, fractional differential equations, simulation techniques, optimal control, and image processing.

Fariba B. Sarand - is currently an Assistant Professor in the Department of Civil Engineering at the Tabriz Branch of Islamic Azad University, Tabriz, Iran. She received her Ph.D. degree in Geotechnical Engineering from the University of Tabriz in 2014. Her research focuses on physical and numerical modeling in geotechnical engineering.